

Modified switching control of SRM drives for electric vehicles application with torque ripple reduction

Sreeram Krishnamoorthy, Preetha Parakkat Kesava Panikkar

Department of Electrical and Electronics Engineering, Amrita Vishwa Vidyapeetham, Amritapuri, India

Article Info

Article history:

Received Apr 19, 2023

Revised Aug 30, 2023

Accepted Sep 16, 2023

Keywords:

Electric vehicle

Machine modeling

Switched reluctance motor

Torque ripple

Traction motor

ABSTRACT

The switched reluctance motor (SRM) offers extensive prospects, particularly within the realm of electric vehicles (EVs). Its robust construction, wide speed range, high torque density, and efficiency provide significant advantages that surpass other motors. Nonetheless, controlling these motors is more intricate when compared to conventional DC brushed or AC motors. This complexity arises due to the non-linear inductance characteristics of SRMs, resulting in undesirable effects like torque ripple, vibrations, and noise. Using the conventional full-bridge inverter, three switching approaches are highlighted for various operating modes of an EV. This aims to reduce costs and the number of switching pulses, leading to a more compact system, elimination of dead time, and switching losses. The MATLAB/Simulink platform was utilized to examine the operational effectiveness of a three-phase 6/4 poles SRM drive. Additionally, this paper focuses on mitigating torque ripple concerns by employing an adaptive neuro-fuzzy inference system (ANFIS) controller that has better efficiency and superior responses compared to conventional controllers such as fuzzy logic control (FLC) and proportional integral (PI) control. The results of the simulation encourage the practical implementation of the system, which is the next step in the author's research.

This is an open access article under the [CC BY-SA](#) license.



Corresponding Author:

Sreeram Krishnamoorthy

Department of Electrical and Electronics Engineering, Amrita Vishwa Vidyapeetham

Amritapuri, India

Email: sreeram@am.amrita.edu

1. INTRODUCTION

Electric vehicles (EVs) have achieved recognition due to their environmentally friendly nature [1]. They have the potential to mitigate greenhouse gas (GHG) emissions, pollution, and noise, while cutting down on fuel costs associated with traditional vehicles [2]. They contribute to the stability of the power grid by integrating renewable energy sources like solar and wind generation to cope with the sudden increases in power demand [3]. A crucial component of the electric vehicle charging system (EVCS) is smart charging, which serves multiple purposes including battery recharging, grid support by providing reactive power compensation, reducing harmonics, and enabling bidirectional power flow with the grid [4]. EVs can enhance the power quality of the utility grid. However, designing EVs comes with significant challenges such as cost, space limitations, flexibility, energy efficiency, and voltage management [5]. For instance, there have been recent advancements in the power electronic converters for EVs, like integrated power converters that have superior efficiency, reduced output ripple, and compact size compared to conventional converters [6]. The motor selection criteria for electric vehicles (EVs) encompass several key design parameters, such as a torque-speed profile, reliability, power-to-weight ratio, efficiency, controller expenses, and overall price [7].

Induction motors (IM) have been widely used in EVs for their simplicity, robustness, and reliability, making them suitable for various automotive applications. They however suffer from lower efficiency at low

speeds, higher weight, reduced power density, limited speed range, and heat generation. permanent magnet synchronous machines (PMSMs) are strong competitors to IM in EVs due to superior torque speed profile, power density, efficiency, and reduced heating. PMSMs have shortcomings such as costly permanent magnet and rare earth dependency which leads to supply chain challenges and cost fluctuations, and the demagnetization issues affects its long term reliability [8].

Switched reluctance motor (SRM) has enormous scope for EVs due to its compact size, robustness, wide speed characteristics, low cost, higher efficiency, and fault tolerance ability [9]. The words in [10], a multi-functional converter was developed for an SRM based EV drives with driving, braking, and battery charging abilities. SRM based EVs can also be used in renewable applications as demonstrated by instances such as the utilization of a hybrid boost switch mode DC-DC converter [11] integrated with a photovoltaic (PV) module. The SRM has the ability to function as either a motor or a generator, depending on the configurations set on the controller. Switched reluctance generator (SRG) has become a highly viable option for wind energy conversion systems (WECS) [12]. Furthermore, in this case, SRGs demand proper parameter selection and robust controllers to accommodate a wide range of speeds. Implementing early fault detection methods for continuous monitoring of wind turbine health can enhance turbine reliability and lead to reduced maintenance costs by identifying issues before they escalate into major failures [13]. Defects taking place inside the motor, like armature phase shorts or opens, are termed internal faults. On the other hand, anomalies occurring in external components like load, excitation sources or the converters, are denoted as external faults [14]. SRMs also have constraints like torque ripple, acoustic noise and vibration compared to PMSMs, which impacts ride comfort and overall vehicle noise levels which might make them less suitable in certain EV applications [15].

Numerous converter configurations have been developed to enhance control techniques, expand performance capabilities, enable fault-tolerant operation, and address other design aspects. The commonly used asymmetric bridge system can function in hard-switching, and soft-switching modes. Its key benefits are flexibility and independent phase control. Challenges may arise in low voltage applications, particularly concerning the demagnetization voltage at high speeds, which can be attributed to the constant voltage supply [16]. Addressing voltage ripple necessitates a sizable capacitor on the voltage source side. Another concern is the possibility of substantial power losses through diodes in the generating mode due to high currents. There have been modifications in this topology with fewer switches as proposed in [17]. The shared phase winding configuration enhances power component utilization, thereby leading to an increased duty cycle and independent phase control [18]. This reduces the switches required while enabling individual control of phase currents. The primary drawbacks are the high SCR losses and expenses for high-power applications, alongside reduced fault tolerance capabilities. The primary benefits associated with Miller converter include reduced power components and the potential for independent phase control. There are limitations including fault tolerance, unwanted circulating currents and excessive electromagnetic fields (EMF) for EV applications [19]. The traditional H-bridge converter reduces conduction and switching losses, resulting in improved efficiency during freewheeling and demagnetization phases [20]. The limitations involve the inadequate utilization of switches and the expenses associated with driver circuits. The C-dump converter enables lesser number of switches with independent phase control. However, it suffers from limited demagnetization voltage and fault tolerance [21]. Similarly, the R-dump converter enables a simple structure, lower cost due to lesser number of switches [22]. The main drawback is its lower efficiency especially for high power cases.

Torque ripple reduction by machine structure optimization involves increasing the number of phases and improving the stator or rotor pole arc and winding connection [23]. Increasing the phase number has an added benefit regarding torque ripple and fault tolerance [24]. However, this increases the device components, escalating the overall cost and adding complexity to the control algorithms. The main cause of torque ripple in SRM is its double salient geometry and current transition from one phase to another. Pole arcing and rotor skewing are some of the mechanical modifications for torque ripple reduction [25]–[28]. SRM's with distinct number of stator and rotor poles, especially with a greater number of rotor poles have been suggested in [29], to decrease the ripple. The rotor structure becomes complex and needs precise design aspects like winding connection, arc angle, and saturation conditions, for high level of optimization [30]. Commonly used torque minimization control techniques include PI controllers for speed and torque ripple control [31]. However, this method is less efficient compared to fuzzy logic and neural control [32].

This paper firstly introduces the standard three phase bridge inverter topology for SRM drive based EV. One advantage of using this configuration is the possibility of a readily available module, without need to change the machine's internal assembly or excitation technique. It can achieve elevated voltages with minimal harmonics, without employing transformers or series-connected synchronized switching components. It can readily deliver the substantial power necessary for a sizable electric propulsion system. The same can be modified into a multilevel topology to reduce the harmonics. In such cases, voltage levels also increases and there are no voltage sharing problems even if series of connected devices are used. It can achieve enhanced

power quality, reduced switching losses, and increased voltage capacity. Additionally, the design characterized by minimized parasitic inductances leads to improved electromagnetic compatibility. Three operating modes are discussed for the converter operation- with the inclusion of dead time, without the dead time and an additional alternate firing scheme which could be used based on various operating modes of an EV. Finally, the ANFIS control for torque ripple reduction is discussed which is more efficient compared to conventionally used PI, fuzzy, and neural control.

This section offers an understanding of how SRM are significant within the context of EV applications and discusses in detail the related work starting with SRM drive based converters for EV application, the various machine design enhancement, and the torque ripple control methods. The next section focuses on the methodology and modeling of the SRM for the analysis followed by the converter operation, operating modes and torque ripple minimization. In the fourth section, a comparison is drawn between converter performance and techniques for reducing torque ripple. The last section wraps up by summarizing the key findings, emphasizing the controller's use cases, and identifying potential areas for enhancement.

2. METHODOLOGY

Electric machine modeling allows for performance analysis before the physical hardware prototype is developed. Utilizing a small-scale or software model proves cost-effective compared to directly designing the actual hardware. MATLAB/Simulink version R2022b is used to model a 6/4 pole SRM [33]. The SRM modeling equation is expressed using stator phase voltage (V), stator resistance (R_s), phase current i (A), flux linkage λ , rotor position θ , speed w_m , and phase inductance L (H).

$$V = iR_s + L(\theta, i) \frac{di}{dt} + iw_m \frac{dL(\theta, i)}{dt} \quad (1)$$

The instant power per phase P_i is computed by multiplying (1) by the instantaneous current.

$$P_i = Vi = i^2 R_s + iL(\theta, i) \frac{di}{dt} + i^2 w_m \frac{dL(\theta, i)}{dt} \quad (2)$$

If T_e is the electromagnetic torque in Nm developed, then as in (3).

$$T_e = \frac{1}{2} i^2 \frac{dL(\theta, i)}{d\theta} \quad (3)$$

It can be inferred that the torque remains uninfluenced by the current's direction and depends exclusively on the rate of inductance parameter change during the switching period. The mechanical torque equation is derived using the motor and load moment of inertia J (kg/m^2), load torque T_L (Nm), angular velocity w_m (rad/s), and viscous friction coefficient D .

$$T_e = Dw_m + T_L + J \frac{dw_m}{d\theta} \quad (4)$$

In the linear model, the inductance changes linearly as the rotor position vary and remain unaffected by the phase current. Hence, a minimum inductance (unaligned inductance) and a maximum inductance (aligned inductance) are considered, with their variation assumed to be linear with respect to the rotor position. The non-linear case is employed for practical scenarios, where the inductance is influenced by both the rotor's position and the phase current. This non-linear approach is more realistic and better represents the behavior of the system in real-world scenarios like EV applications. The (1)-(4) are used to construct the Simulink model in MATLAB [34]. In the context of EV applications, the SRM drive, along with an appropriate control technique, plays a critical role in delivering the necessary electrical outputs to the machine windings, making it a pivotal component affecting the overall performance of the EV. To facilitate winding excitation and commutation, various converters are utilized, including asymmetric, integrated battery chargers, C-dump, bifilar, Miller converter, resonant converters, among others. The choice of converter type has an impact on factors such as the number of switches, cost, drive size, efficiency, power quality, and torque ripple. The widely employed SRM drive controllers, such as PI and fuzzy logic, are compared with ANFIS control by simulation in MATLAB software. The key aspects analyzed for performance evaluation include torque, ripple content, and speed response. For comparison purposes, the simulation parameters for the SRM motor drive are assumed to be as shown in Table 1.

Table 1. Design ratings of the SRM drive

Parameters	Values	Parameters	Values
Switched reluctance motor (SRM)	No. of stator pole - 6 No. of rotor pole - 4 6/4 three-phase SRM	Stator phase voltage	240 V
Stator Pole arc	32°	Stator inductance (H)	960
Rotor Pole arc	45°	Reference speed	1500 rpm
Aligned inductance (H)	0.02	Reference or maximum current	200 A
Unaligned inductance (H)	0.0006	Hysteresis band limits	+/-10 A
Maximum flux linkage (Wb)	0.5	Stator resistance	0.05 ohm
Inertia (kg.m ²)	8.9e-3	Turn on angle	45°
Friction (Nms)	0.005	Turn off angle	75°

3. SRM DRIVE BASED ON BRIDGE INVERTER

A significant characteristic of the standard inverter is that it allows both magnetizing and demagnetizing voltages to attain the level of the DC-bus voltage simultaneously while being applied during the conduction overlap in the adjacent phases of the SRM. Additionally, the voltage across the power switches matches the DC-bus voltage. The SRM phases are connected in star configuration enabling bipolar current flow as shown in Figure 1.

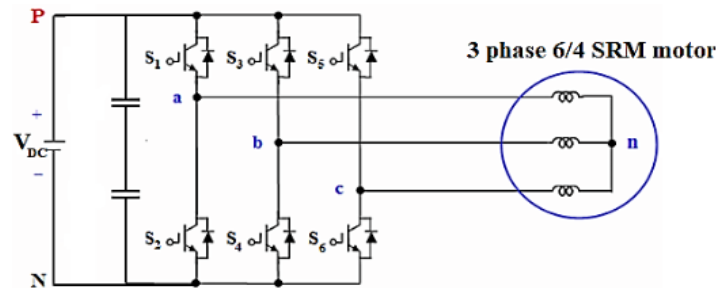


Figure 1. Power converter circuit for the SRM drive

3.1. Normal operating mode with dead time

The conventional switching strategy for three-phase full-bridge converter based SRM drive is depicted in Figure 2. For the positive slope of the phase inductance, the upper switches (S_1 , S_3 , and S_5) are triggered to allow current flow into the respective phase. The negative return current flows to the following phase winding which is turned on by switching the lower ones (S_2 , S_4 , and S_6). This sequential switching sequence repeats every 30 degrees. During these transitions, an immediate shift in the phase current's polarity occurs, wherein the lower switch turns off as the upper switch turns on. If the dead-time value is insufficiently set, the possibility of shoot-through issues emerges. This, in turn, introduces torque fluctuations and fluctuations in the DC-link current and voltage, ultimately impacting the motor drive's performance. To avoid the shoot-through fault and its associated issues, the introduction of dead-time is necessary. The switching transitions are depicted in Table 2. The control techniques to reduce torque ripples are discussed in the upcoming sections.

Table 2. Switching pattern for the SRM drive

	Rotor angle (Mechanical)	Switches (ON)	Polarity of I_a	Polarity of I_b	Polarity of I_c
Conventional switching strategy	0-30°	S_3, S_6	0	+	-
	30-60°	S_2, S_5	-	0	+
	60-90°	S_1, S_4	+	-	0
	90-120°	S_3, S_6	0	+	-
	120-150°	S_2, S_5	-	0	+
	150-180°	S_1, S_4	+	-	0
Modified switching strategy	0-30°	S_4, S_5	0	-	+
	30-60°	S_2, S_5	-	0	+
	60-90°	S_2, S_3	-	+	0
	90-120°	S_3, S_6	0	+	-
	120-150°	S_1, S_6	+	0	-
	150-180°	S_1, S_4	+	-	0

3.2. Modified switching operation without dead time

This switching strategy involves two switches in the same converter leg, alternating their commutation during each electrical cycle with zero dead time between switching transitions. During the positive or flat slope of the phase inductances, two switches are simultaneously activated. This facilitates current flow through both phase windings, with one phase carrying positive current and the other bearing negative current. Consequently, turn on duration is now twice compared to the traditional switching method as given in Figure 2. This leads to a 50% reduction in the switching frequency for each switch, thereby proportionally lowering switching losses. Furthermore, this adjustment eliminates the necessity for immediate shifts in current polarity, thereby preventing any dead-time-related issues. The torque remains unaffected since it remains independent of the current's direction.

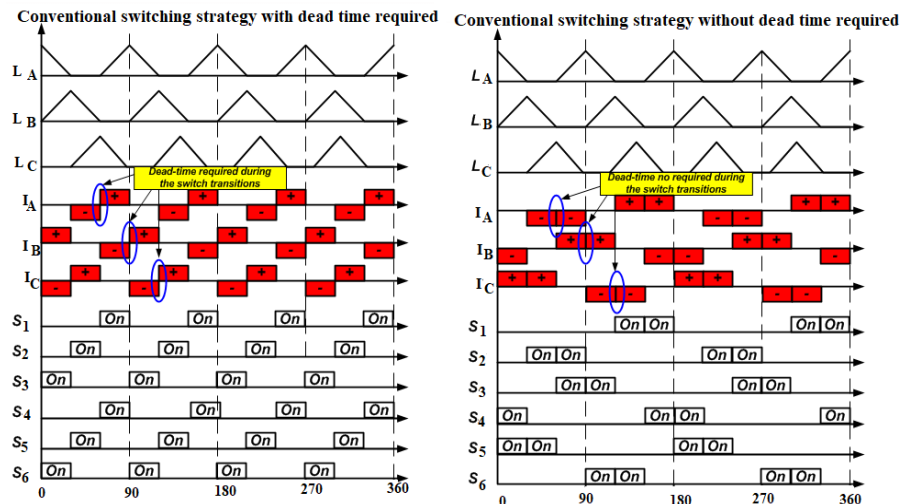


Figure 2. Switching waveforms for the SRM drive

3.3. Alternate firing scheme

The stator undergoes multiple magnetization cycles in a single 360° motor rotation cycle on excitation by the phase currents. For high-speed applications including EVs, there are different operating modes such as start-up or full throttle acceleration, light load/heavy load conditions, braking/deceleration, cruising/normal driving, regeneration. For few modes such as normal driving or cruising mode, it would not be effective to have the motor control unit fire several times during each revolution as this could lead to high switching rates, resulting in huge losses. Thus, it might be better to energize the motor with more power for lesser excitations instead of lower power for numerous excitations. Operating a motor in high power state might enable it to run with better efficiency compared to low power mode. The motor's output power depends on the winding current in each cycle. The power is only supplied every alternate rotation rather than every rotation. The gate cutter mechanism excites the stator coils with more current during these alternate numbers of rotations. The gate blocking or interrupter module is independent of the motor drive and control logic and can be added or removed at will without needing to modify or replace the original drive as shown in Figure 3.

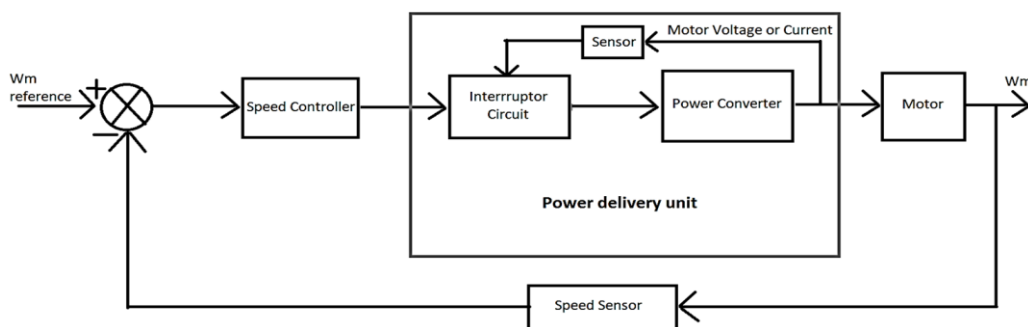


Figure 3. Gate signal blocking action

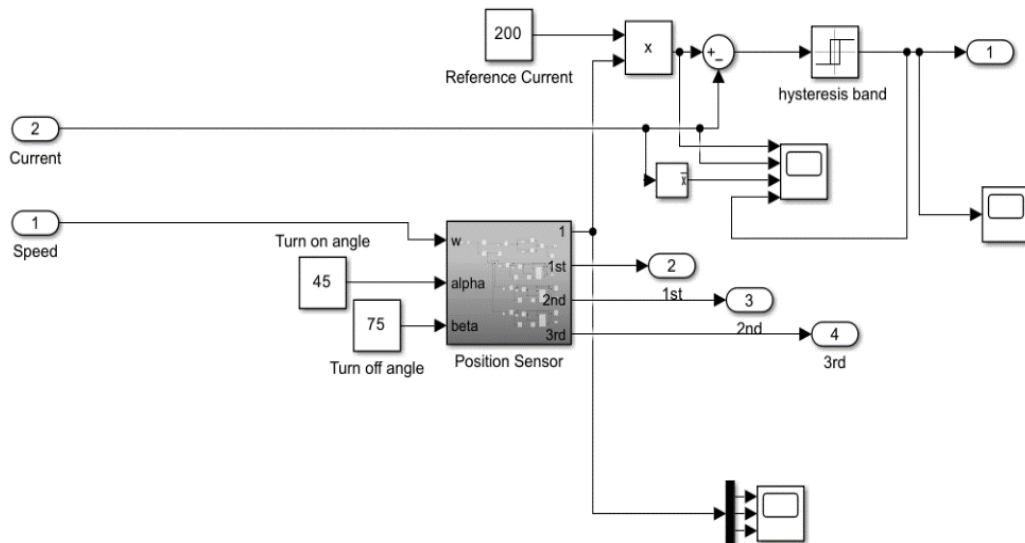


Figure 6. PI Hysteresis control unit

3.5. Torque ripple reduction based on fuzzy control

During transient cases, the fuzzy logic controller (FLC) outperforms the PI regulator in terms of response and efficiency. The FLC receives two inputs: speed error (E) and rate of change in speed error (CE). The FLC generates its output as follows: $u(k) = F[E(k) - CE(k)]$.

In the first step, crisp inputs are transformed into linguistic variables through fuzzification as given in Figure 7. The second step involves defining rules, as illustrated in Table 3. The FLC's rule base generates the desired output as linguistic variables. The last step called defuzzification, involves converting these linguistic variables into outputs. Figures 8-10 shows the membership functions for the error change in error of motor speed, and output of SRM. The error is restricted within the range of -1 to 1 using a saturation unit. Based on the final speed output, the gate signals are produced. A Mamdani type FLC was chosen as it is the most widely used type and has the ability to reduce steady state error to zero [36].

Table 3. FLC rules

		Change in error						
Error		NL	NM	NS	Z	PS	PM	PL
NL		NL	NL	NL	NL	NM	NS	Z
NM		NL	NL	NL	NM	NS	Z	PS
NS		NL	NL	NM	NS	Z	PS	PM
Z		NL	NM	NS	Z	PS	PM	PL
PS		NM	NS	Z	PS	PM	PL	PL
PM		NS	Z	PS	PM	PL	PL	PL
PL		Z	PS	PM	PL	PL	PL	PL

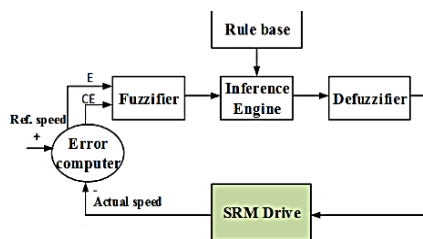


Figure 7. FLC based SRM drive

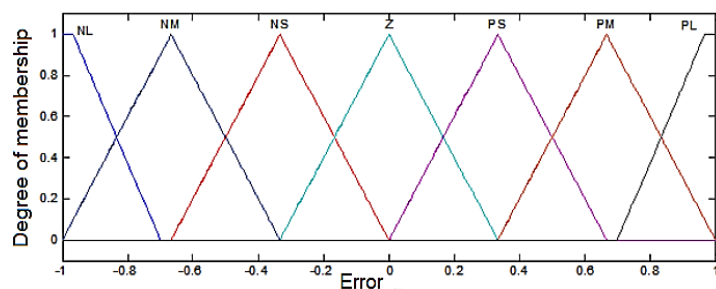


Figure 8. Membership function for error in speed

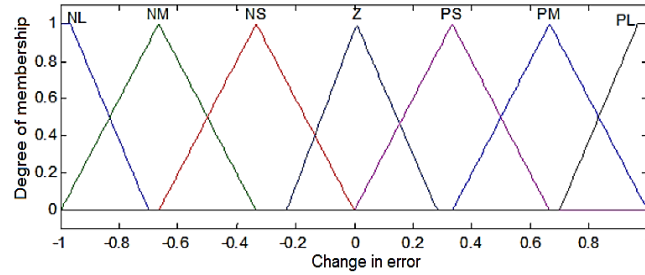


Figure 9. Membership function for change in error

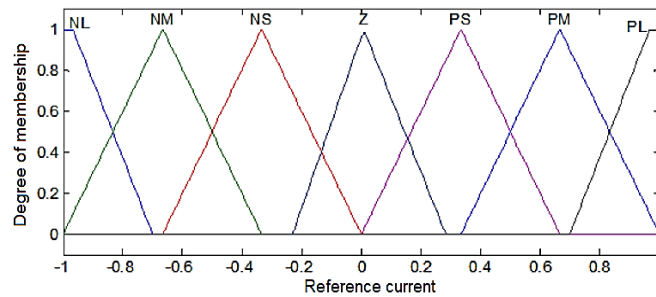


Figure 10. Output variable for SRM motor

3.6. Torque ripple minimization by ANFIS controller

The ANFIS current compensator is proposed for reducing the torque ripple and subsequent acoustic noise effects as shown in Figure 11. The adaptive node is represented by the square element, while the fixed node is denoted by the circular element. The controller adds extra current to each phase current to mitigate torque ripple in the areas where torque decreases. It also decreases speed estimation error. By clubbing the merits of the fuzzy inference scheme and the learning skill of neural networks, the drive gives a better dynamic response than its PI counterpart. The structure comprises five layers: fuzzy layer, product layer, normalization layer, defuzzy layer, and summation layer. The controller produces a gate trigger signal for the converter centered on the inputs-speed error and changes in the speed error. The input variables for fuzzification are fed into the rule-based unit, which is linked to the neural network unit. The back propagation algorithm is employed for selecting a suitable set for the rule base. The torque and current ripples are less, and the speed response is better compared to the PI controller. This is beneficial in EVs where quick response is necessary. The inner loop controls the current and outer loop regulates the speed. The ANFIS-based speed controller derives the reference current from the speed error signal. Subsequently, the ANFIS-based current regulator compares the measured current with the reference current, producing the output signals for the PWM to turn ON the converter switches. The converter, in turn, manages both the speed and current through the standard functioning of the SRM windings.

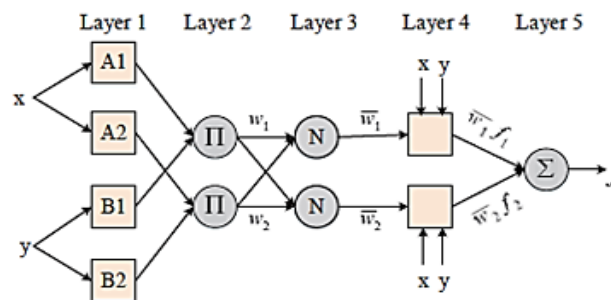


Figure 11. ANFIS structure

4. RESULTS AND DISCUSSION

Initially, due to the small motor EMF, the stator current is quickly regulated to its reference value. The average torque is almost proportional to the reference current; hence, this mode is called constant torque or current-controlled operation. For higher speeds, the back EMF usually increases; therefore, currents cannot reach the reference provided by the existing regulators. This is voltage-fed mode as there is no modulation of the power switches, and average torque varies inversely with the motor speed. The error is significant when the current speed deviates from the reference speed or when disturbances arise. The turn ON and OFF angles are computed with equations that depend on the actual speed, and reference current. After the speed error is rectified, efficiency optimization occurs by controlling the peak current. The actual winding current is sampled and compared with the former sampled current. The PI control regulates the motor speed. The output torque waveform in Figure 12 shows that output torque has a high ripple or noise component, which directly affects the power and causes vibration. For the regular operation of the SRM drive, the current, torque, flux, and speed are continuous for the time period as depicted in Figure 12.

In the gate blocking mode, the respective outputs become zero during periodic intervals of time, as indicated in Figure 13. During those rotations with the gate blocked, the motor freewheels. Phase voltages and currents reduce gradually during the gate blocking period, which causes the electromagnetic torque and flux to become lesser. In order to achieve the same motor speed for a set load, the load current during the phase firings would be higher in as the motor is only powered every other rotation. Electric motors are the most efficient when operating near or at their rated capacity and this control logic would enable the motor to operate within that high efficiency zone by enabling high power action in bursts rather than continuous low or medium power action. As a result, the efficiency should theoretically increase as the motor is running closer to its rated current. This approach could also be employed by high-RPM EV motors to ensure their operation within the optimal torque-speed range, thereby maximizing efficiency.

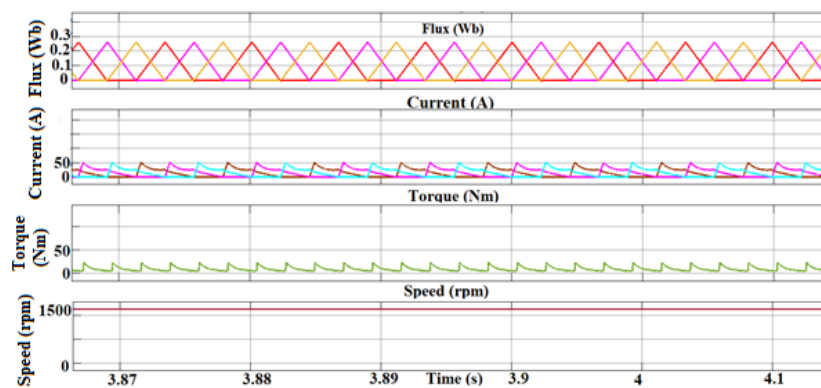


Figure 12. SRM output waveforms during normal operation

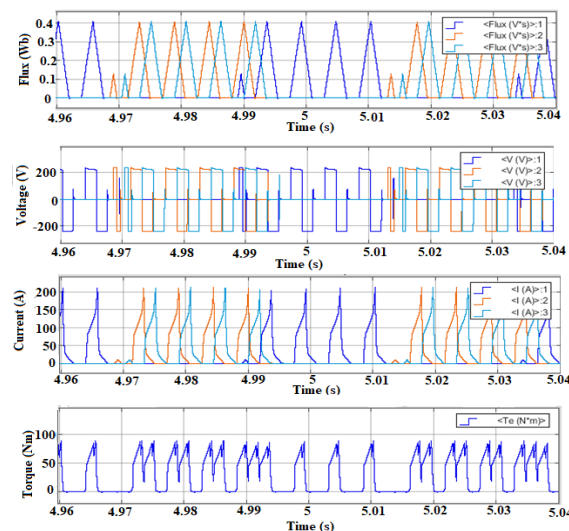


Figure 13. Output waveforms during gate blocking mode

Figure 14 displays the motor speed under both PI control and FLC for gate blocking mode. Parameters such as rise time (the duration for the motor to reach 90% of the reference speed), settling time (time taken to settle down to the reference speed), and the deviation between actual speed and reference speed were compared. The PI control requires 1.2 second to stabilize at the reference speed, while the FLC achieves this in 0.4 seconds as outlined in Table 4. For PI control, a minor overshoot of around 0.4 seconds is observed when the motor speed reaches 1500 rpm. This brief instance of overshoot, could potentially impact the motor controller's effectiveness. Both cases exhibit nearly identical rise times, with a marginal advantage in favor of FLC and FLC has almost nil steady state error compared to PI control. In conclusion, the suitability of FLC for the SRM drive is established, showcasing its capacity to provide a smooth speed response across a broad range of speeds. At high rpm speeds (above 2000 RPM), variations in torque are not a significant issue as the vibrations are usually relatively minor. For low rpm, high load conditions, the torque fluctuations become very pronounced and can result in additional stresses to the machinery. As such, this strategy works best for low load high rpm cases. The gate blocking mechanism can be more effective if a suitable torque ripple minimization technique can be incorporated into the controller.

Noise, disturbances, and variations in load torque ripple can influence the performance, current and speed of the SRM drive. It uses a neural controller, including a fuzzy controller and a feed-forward neural network, to produce the output control signals (turn-on angle, turn-off angle, and peak current) to regulate the energy flow in the SRM. For the ANFIS scheme, rotor position and stator phase current are the controller input and output respectively. The torque estimator computes the instantaneous torque to fix the controller membership function. The machine parameters like flux, torque, and current are shown in Figure 15. The Neuro-fuzzy based SRM drive control produces a torque profile in Figure 16 with a lesser ripple compared to the previous cases. It is possible to achieve lower torque and current distortion in addition to fast dynamic and torque, and flux response. Due to the lower ripple content, the average torque is higher. Due to smaller vibration, the speed settles down faster to its steady state value as indicated in Figure 17 compared to conventionally used PI and Fuzzy control. The main benefit is that there is no requirement for an analytical system model and they are apt for nonlinear systems, as it is independent of the machine parameters. The adaptive learning approach results in robust performance even with parameter deviation and load disturbance. Due to the ANFIS compensator's ability to learn, the control is more flexible and has machine independent characteristics. If the system's load, voltage supply, or operating speed changes, the compensator automatically configures to perform at this new operating point and seek for the necessary torque oscillation minimization.

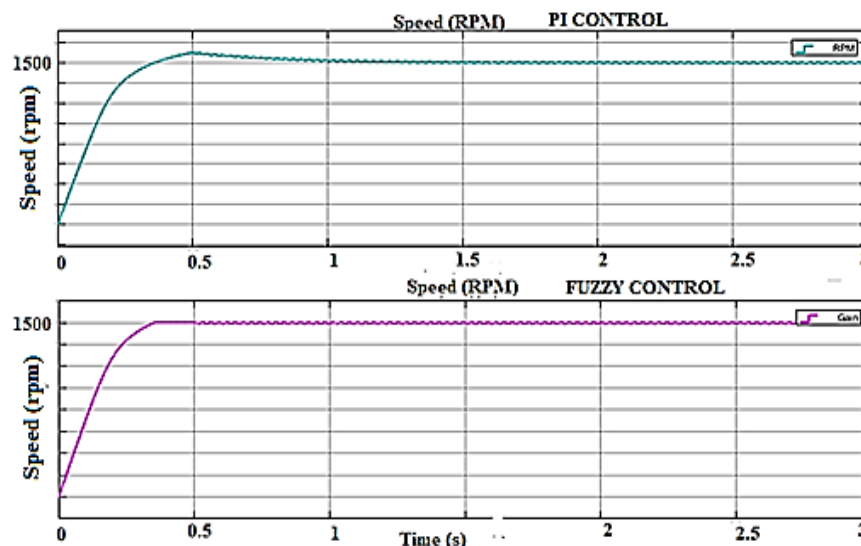


Figure 14. Speed response using PI and FLC with gate blocking mode

Table 4. PI control and FLC evaluation using gate blocking mode

Reference speed=1500 rpm	PI Control	Fuzzy Logic Control
Rise time (seconds)	0.4	0.3
Settling time (seconds)	1.2	0.4
Steady state error (%)	0.28	0.05

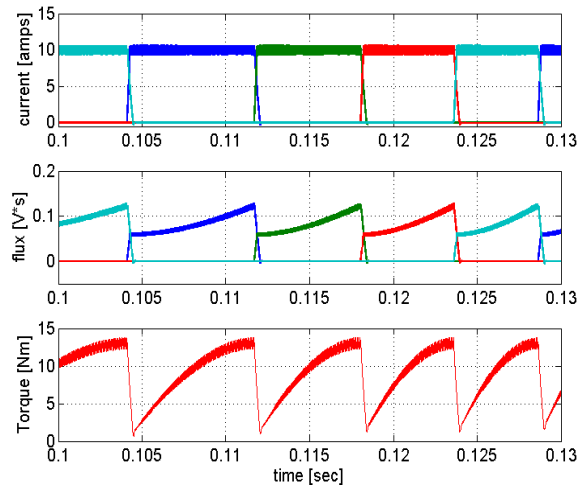


Figure 15. Output waveforms using ANFIS control

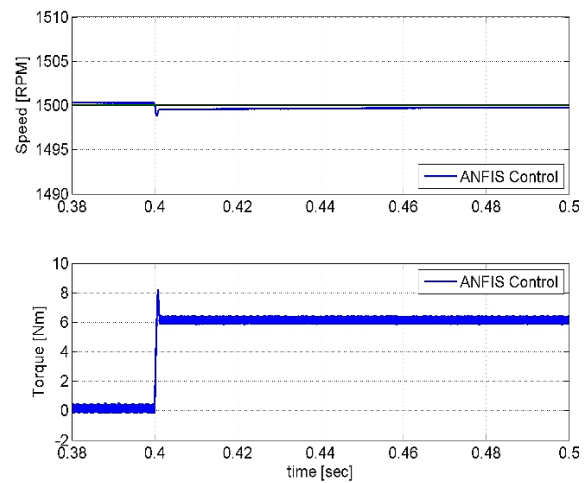


Figure 16. Output speed and torque using ANFIS control

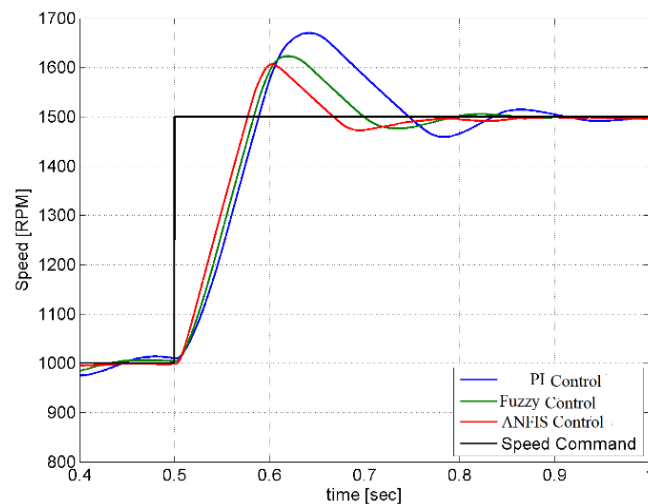


Figure 17. Comparison of speed response for the controllers

5. CONCLUSION

Switched reluctance motor will have extensive applications in EVs, industrial and domestic drives, servo drives, and aircraft applications once their main shortcomings of torque ripples and noise are overcome. The key aim of utilizing the standard three-phase full-bridge converter is to decrease the overall drive expenses and potentially open up new possibilities for standard voltage source inverters (VSI) in SRMs to compete with other AC motors. The entire DC-bus voltage is accessible for both the magnetization and demagnetization, even for overlapping currents during simultaneous conduction of two phases. Owing to the reduced components (assuming a three-phase VSI 6-pack unit), installation and manufacturing is simpler. Two additional switching strategies are discussed for the above converter other than the conventional switching. The second strategy eliminates the requirement for dead time during commutation, thus reducing the switching losses. The third switching technique based on alternate firing was proven and the fuzzy logic approach achieved stabilization towards the reference speed more rapidly compared to the PI controller, a crucial aspect for EVs. For practical cases, a cost study must be performed to check if such a unit as an add-on module is possible with a controller would be to determine the timing. The multiple operating modes enable the SRM to serve a broader range of applications and even replace PMSM and IM motors. The ANFIS control technique offers better speed response and torque characteristics compared to existing PI, fuzzy and neural controllers as discussed in the results section. Further research can be concentrated on the following aspects: i) Similar to SRMs, synchronous reluctance motors are also appealing due to their durability, efficiency, minimal ripple, and control and the same proposed control technique can be adopted; ii) The radial noise and torque ripple

must be limited without impacting torque density and performance; iii) The SRM drive must be designed by optimizing the converter topology and control techniques instead of modifying the stator and rotor assemblies to reduce production difficulty and cost; and iv) Further fine tuning of control schemes including sensorless control techniques to minimize the vibrations and torque ripple must be designed for fault tolerance and for a wide speed range.

ACKNOWLEDGEMENTS

The authors would like to express their gratitude to Amrita Vishwa Vidyapeetham, Amritapuri, India, for providing this research grant and support.




REFERENCES

- [1] K. Sreeram, P. K. Preetha, and P. Poornachandran, "Electric Vehicle Scenario in India: Roadmap, Challenges and Opportunities," in *2019 IEEE International Conference on Electrical, Computer and Communication Technologies (ICECCT)*, Feb. 2019, pp. 1–7, doi: 10.1109/ICECCT.2019.8869479.
- [2] A. Rabie, A. Ghanem, S. S. Kaddah, and M. M. El-Saadawi, "Electric vehicles based electric power grid support: a review," *International Journal of Power Electronics and Drive Systems*, vol. 14, no. 1, pp. 589–605, 2023, doi: 10.11591/ijpeds.v14.i1.pp589-605.
- [3] R. S. Sreelekshmi, R. Anusree, V. Raveendran, and M. G. Nair, "Solar Fed Hybrid Energy Storage System in An Electric Vehicle," *2018 9th International Conference on Computing, Communication and Networking Technologies, ICCCNT 2018*, 2018, doi: 10.1109/ICCCNT.2018.8493846.
- [4] V. Raveendran, C. Alvarez-Bel, and M. G. Nair, "Assessing the ancillary service potential of electric vehicles to support renewable energy integration in touristic islands: A case study from Balearic island of Menorca," *Renewable Energy*, vol. 161, pp. 495–509, 2020, doi: 10.1016/j.renene.2020.06.083.
- [5] V. Raveendran and M. G. Nair, "Power factor corrected level-1 DC public green-charging infrastructure to promote mobility in India," *IET Power Electronics*, vol. 13, no. 2, pp. 221–232, 2020, doi: 10.1049/iet-pel.2019.0009.
- [6] K. Sreeram, S. Surendran, and P. K. Preetha, "A Review on Single-Phase Integrated Battery Chargers for Electric Vehicles," *Lecture Notes in Networks and Systems*, vol. 401, pp. 751–765, 2023, doi: 10.1007/978-981-19-0098-3_71.
- [7] A. A. E. B. A. El Halim, E. H. E. Bayoumi, W. El-Khattam, and A. M. Ibrahim, "Electric vehicles: a review of their components and technologies," *International Journal of Power Electronics and Drive Systems*, vol. 13, no. 4, pp. 2041–2061, 2022, doi: 10.11591/ijpeds.v13.i4.pp2041-2061.
- [8] B. Bilgin *et al.*, "Making the Case for Switched Reluctance Motors for Propulsion Applications," *IEEE Transactions on Vehicular Technology*, vol. 69, no. 7, pp. 7172–7186, 2020, doi: 10.1109/TVT.2020.2993725.
- [9] Y. Lan *et al.*, "Switched reluctance motors and drive systems for electric vehicle powertrains: State of the art analysis and future trends," *Energies*, vol. 14, no. 8, 2021, doi: 10.3390/en14082079.
- [10] D. Kalpana, M. K. Kumar, and P. Tripura, "A multi-functional converter based switched reluctance motor drive for electric vehicle," *International Journal of Power Electronics and Drive Systems*, vol. 13, no. 4, pp. 1975–1983, 2022, doi: 10.11591/ijpeds.v13.i4.pp1975-1983.
- [11] R. K. Dasari and D. G. Immanuel, "Photovoltaic hybrid boost converter fed switched reluctance motor drive," *International Journal of Power Electronics and Drive Systems*, vol. 13, no. 1, pp. 275–288, 2022, doi: 10.11591/ijpeds.v13.i1.pp275-288.
- [12] F. P. Scalcon, G. Fang, C. J. V. Filho, H. A. Grundling, R. P. Vieira, and B. Nahid-Mobarakeh, "A Review on Switched Reluctance Generators in Wind Power Applications: Fundamentals, Control and Future Trends," *IEEE Access*, vol. 10, pp. 69412–69427, 2022, doi: 10.1109/ACCESS.2022.3187048.
- [13] M. El Mahfoud, B. Bossoufi, N. El Ouanjli, S. Mahfoud, M. Yessief, and M. Taoussi, "Speed Sensorless Direct Torque Control of Doubly Fed Induction Motor Using Model Reference Adaptive System," *Lecture Notes in Networks and Systems*, vol. 211 LNNS, pp. 1821–1830, 2021, doi: 10.1007/978-3-030-73882-2_165.
- [14] I. Husain, A. Radun, and J. Nairus, "Fault analysis and excitation requirements for switched reluctance-generators," *IEEE Transactions on Energy Conversion*, vol. 17, no. 1, pp. 67–72, Mar. 2002, doi: 10.1109/60.986439.
- [15] K. Diao, X. Sun, G. Lei, Y. Guo, and J. Zhu, "Multimode Optimization of Switched Reluctance Machines in Hybrid Electric Vehicles," *IEEE Transactions on Energy Conversion*, vol. 36, no. 3, pp. 2217–2226, 2021, doi: 10.1109/TEC.2020.3046721.
- [16] V. F. Pires, A. J. Pires, A. Cordeiro, and D. Foito, "A Review of the Power Converter Interfaces for Switched Reluctance Machines," *Energies*, vol. 13, no. 13, 2020, doi: 10.3390/en13133490.
- [17] A. K. Kolluru and M. K. Kumar, "Closed-loop speed control of switched reluctance motor drive fed from novel converter with reduced number of switches," *International Journal of Power Electronics and Drive Systems (IJPEDS)*, vol. 11, no. 1, pp. 189–199, Mar. 2020, doi: 10.11591/ijpeds.v11.i1.pp189-199.
- [18] C. Gan, J. Wu, Y. Hu, S. Yang, W. Cao, and J. M. Guerrero, "New Integrated Multilevel Converter for Switched Reluctance Motor Drives in Plug-in Hybrid Electric Vehicles with Flexible Energy Conversion," *IEEE Transactions on Power Electronics*, vol. 32, no. 5, pp. 3754–3766, 2017, doi: 10.1109/TPEL.2016.2583467.
- [19] V. Shah and S. Payami, "An Integrated Driving/Charging Four-Phase Switched Reluctance Motor Drive With Reduced Current Sensors for Electric Vehicle Application," *IEEE Journal of Emerging and Selected Topics in Power Electronics*, vol. 10, no. 6, pp. 6880–6890, 2022, doi: 10.1109/JESTPE.2021.3120468.
- [20] Y. He, Y. Tang, H. Xie, F. Wang, J. Rodriguez, and R. Kennel, "Single-Phase H-Bridge Rectifier Fed High-Speed SRM System Based on Integrated Power Control," *IEEE Transactions on Energy Conversion*, vol. 38, no. 1, pp. 519–529, 2023, doi: 10.1109/TEC.2022.3203626.
- [21] B. P. Reddy, P. R. Bhimireddy, and S. Keerthipati, "A sense winding system and dynamic current profiling to reduce torque ripple of SRM," *International Transactions on Electrical Energy Systems*, vol. 30, no. 2, 2020, doi: 10.1002/2050-7038.12261.
- [22] Vuddanti Sandeep; Vinod Karknalli; and Surender Reddy Salkuti, "Design and comparative analysis of three phase, four phase and six phase switched reluctance motor topologies for electrical vehicle propulsion," *Bulletin of Electrical Engineering and Informatics*, vol. 10, no. 3, pp. 1495–1504, 2021, doi: 10.11591/eei.v10i3.3054.




- [23] M. Abdalmagid, E. Sayed, M. H. Bakr, and A. Emadi, "Geometry and Topology Optimization of Switched Reluctance Machines: A Review," *IEEE Access*, vol. 10, pp. 5141–5170, 2022, doi: 10.1109/ACCESS.2022.3140440.
- [24] T. Das Gupta, K. Chaudhary, R. M. Elavarasan, R. K. Saket, I. Khan, and E. Hossain, "Design modification in single-tooth winding double-stator switched reluctance motor for torque ripple mitigation," *IEEE Access*, vol. 9, pp. 19078–19096, 2021, doi: 10.1109/ACCESS.2021.3052828.
- [25] S. D. Huang, G. Z. Cao, Y. Peng, C. Wu, D. Liang, and J. He, "Design and Analysis of a Long-Stroke Planar Switched Reluctance Motor for Positioning Applications," *IEEE Access*, vol. 7, pp. 22976–22987, 2019, doi: 10.1109/ACCESS.2019.2899038.
- [26] Y. Zhou, J. Jiang, Y. Sun, and P. Hu, "Principles and Implementation of a Novel Radial-Anti-Disturbance Bearingless Switched Reluctance Motor," *IEEE Access*, vol. 9, pp. 162743–162755, 2021, doi: 10.1109/ACCESS.2021.3130294.
- [27] Q. Sun, J. Wu, C. Gan, C. Shi, and J. Guo, "DSSRM Design with Multiple Pole Arcs Optimization for High Torque and Low Torque Ripple Applications," *IEEE Access*, vol. 6, pp. 27166–27175, 2018, doi: 10.1109/ACCESS.2018.2834901.
- [28] G. Davarpanah and J. Faiz, "A Novel Structure of Switched Reluctance Machine with Higher Mean Torque and Lower Torque Ripple," *IEEE Transactions on Energy Conversion*, vol. 35, no. 4, pp. 1859–1867, 2020, doi: 10.1109/TEC.2020.2990914.
- [29] K. Diao, X. Sun, G. Lei, G. Bramerdorfer, Y. Guo, and J. Zhu, "System-Level Robust Design Optimization of a Switched Reluctance Motor Drive System Considering Multiple Driving Cycles," *IEEE Transactions on Energy Conversion*, vol. 36, no. 1, pp. 348–357, 2021, doi: 10.1109/TEC.2020.3009408.
- [30] N. Abdulah, F. A. A. Shukor, R. N. F. K. R. Othman, S. R. C. Ahmad, and N. A. M. Nasir, "Modelling methods and structure topology of the switched reluctance synchronous motor type machine: a review," *International Journal of Power Electronics and Drive Systems*, vol. 14, no. 1, pp. 111–122, 2023, doi: 10.11591/ijpeds.v14.i1.pp111-122.
- [31] P. S. Rekha and T. Vijayakumar, "Torque ripple and noise control of switched reluctance motor using an adaptive fuzzy pi control with the aid of ar algorithm," *International Journal of Power Electronics and Drive Systems*, vol. 12, no. 2, pp. 1239–1251, 2021, doi: 10.11591/ijpeds.v12.i2.pp1239-1251.
- [32] G. Fang, F. Pinarello Scalton, D. Xiao, R. Vieira, H. Grundling, and A. Emadi, "Advanced Control of Switched Reluctance Motors (SRMs): A Review on Current Regulation, Torque Control and Vibration Suppression," *IEEE Open Journal of the Industrial Electronics Society*, vol. 2, pp. 280–301, 2021, doi: 10.1109/OJIES.2021.3076807.
- [33] D. K. Yankov and T. G. Grigorova, "A nonlinear model for a three-phase 12/8 switched reluctance machine," *International Journal of Power Electronics and Drive Systems*, vol. 13, no. 3, pp. 1576–1587, 2022, doi: 10.11591/ijpeds.v13.i3.pp1576-1587.
- [34] K. Sreeram, N. K. Pillai, N. Reddy Marri, T. K. Baiju, and P. K. Preetha, "Simulation of High Efficiency Switched Reluctance Motor (SRM) Drive Control Scheme by Alternate Rotation Motor Firing," *Proceedings of the 2022 3rd International Conference on Intelligent Computing, Instrumentation and Control Technologies: Computational Intelligence for Smart Systems, ICICICT 2022*, pp. 1381–1386, 2022, doi: 10.1109/ICICICT54557.2022.9917825.
- [35] D. F. Valencia, R. Tarvirdilu-Asl, C. Garcia, J. Rodriguez, and A. Emadi, "A review of predictive control techniques for switched reluctance machine drives. Part I: Fundamentals and current control," *IEEE Transactions on Energy Conversion*, vol. 36, no. 2, pp. 1313–1322, 2021, doi: 10.1109/TEC.2020.3047983.
- [36] V. R. Kota, S. Adapa, and J. Ramayya, "Speed control of Switched Reluctance Motor using Fuzzy Logic Controller," *International Journal of Pure and Applied Mathematics*, vol. 120, no. 6, pp. 631–643, 2018.

BIOGRAPHIES OF AUTHORS



Sreeram Krishnamoorthy    completed B.Tech in Electrical and Electronics Engineering and Master's degree in Industrial Drives and Control from Rajagiri School of Engineering and Technology under APJ Abdul Kalam Technological University, Trivandrum. He's pursuing Ph.D. under the guidance of Dr. Preetha P K, Associate Professor, Department of Electrical and Electronics Engineering, Amrita School of Engineering, Amritapuri. He has five international Journal publications to his credit. He has also presented papers in National and International conferences. He has also won three IEEE best awards. His interest areas are power electronics, electric vehicles (EV), electrical machines, and power quality. He can be contacted at email: sreeram@am.amrita.edu.



Preetha Parakkat Kesava Panikkar    completed B. Tech in Electrical & Electronics Engineering and M. Tech. in Power Systems from College of Engineering, Trivandrum, in the year 1995 and 1997 respectively. She obtained her Ph.D. from Amrita Vishwa Vidyapeetham, Amritapuri. Dr. Preetha PK currently serves as Associate Professor and Vice Chairperson at the Department of Electrical and Electronics Engineering at Amrita School of Engineering, Amritapuri. Dr. Preetha is a member of IEEE and a lifetime member of ISTE. She was conferred with the Certificate of Appreciation for her achievements during the academic year 2014-2015 from Amrita Vishwa Vidyapeetham, Amritapuri. She has published many Journals and conference papers to his credit. Her research interest areas include power quality, power system control, and electric vehicles (EV). She can be contacted at email: preethapk@am.amrita.edu.